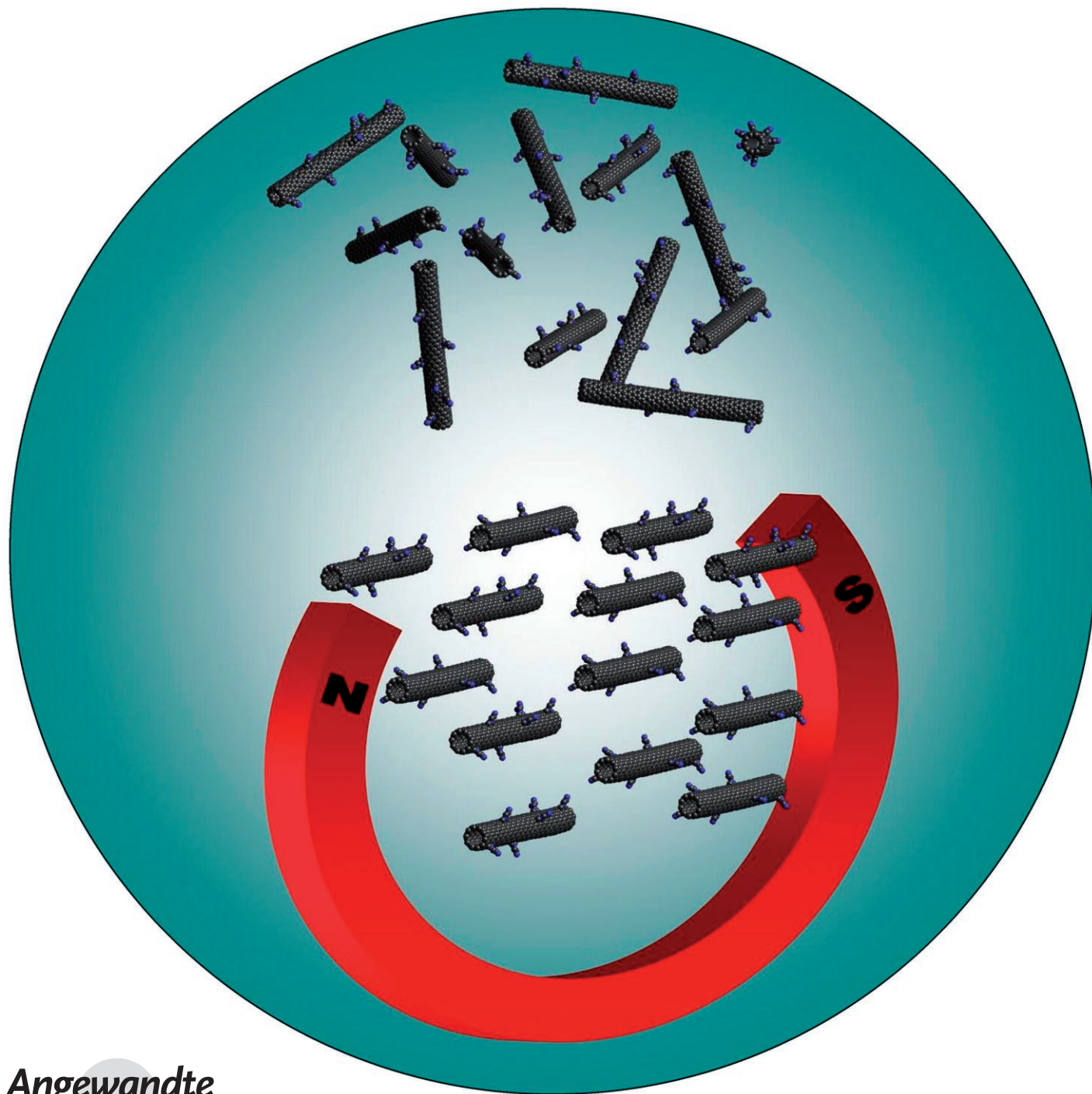


# Alignment of Carbon Nanotubes in Weak Magnetic Fields\*\*

John Tumpene,\* Nikolaos Karousis, Nikos Tagmatarchis, and Bengt Nordén



Alignment of carbon nanotubes is essential for their potential use as a durable nanomaterial, in which bulk properties, such as tensile strength, bending modulus, conductivity, etc., which are dictated by the nanotube long axis, can be amplified by parallel alignment.<sup>[1]</sup> Orientation of diamagnetic molecules in the presence of a magnetic field is a well-known phenomenon for organized structures, such as crystalline solids,<sup>[2]</sup> and even for large systems, such as red blood cells.<sup>[3]</sup> The response of carbon nanotubes to magnetic fields and their alignment with the nanotube long-axis parallel to the field direction has clearly been demonstrated, albeit at relatively high field strengths.<sup>[4–6]</sup> Herein we show the orientation of modified single-walled carbon nanotubes (SWCNTs) in fields up to two orders of magnitude weaker than previously used and therefore in the range of fields commonly available in a standard laboratory (0.1 T). Furthermore, the level of alignment achieved at these low field strengths is very high.

The response of a molecule to a magnetic field can be attributed to the magnetic susceptibility anisotropies of such molecules;<sup>[5]</sup> that is, the magnetic susceptibility parallel to the molecular axis,  $\chi_{\parallel}$ , is different to the perpendicular susceptibility  $\chi_{\perp}$ . Alignment in a magnetic field will depend on the balance between the magnetic energy gain owing to alignment and the thermal energy gain owing to disorder:

$$\frac{(|\chi_{\parallel} - \chi_{\perp}|)H^2}{2} > k_B T \quad (1)$$

where  $k_B$  is the Boltzmann constant,  $T$  the temperature and  $H$  the magnitude of the magnetic field strength. Ajiki et al. have predicted the difference in susceptibilities for SWCNTs to be as great as one order of magnitude. Although this has not yet been evidenced in experimental observations,<sup>[5,7–10]</sup> the most likely reason being cited as the effect of bundling, which will reduce the apparent differential susceptibility. By using more soluble nanotubes, we hoped to fully utilize the extreme differences in susceptibilities to achieve alignment at much lower field strengths. It is possible that the presence of some iron catalyst impurities may contribute to the alignment,<sup>[10]</sup> although we will discuss this possibility below.

The electronic spectroscopy of carbon nanotubes is still poorly understood, with the transitions in the UV/Vis/NIR regions largely masked by scattering artifacts. The fact that nanotube transitions extend in principle uninterrupted across this wide interval also makes their interpretation cumbersome. The presence of fine-structure is, however, well-known and arises from van Hove singularities in the density of states (Figure 1). The probability of an electronic transition, and

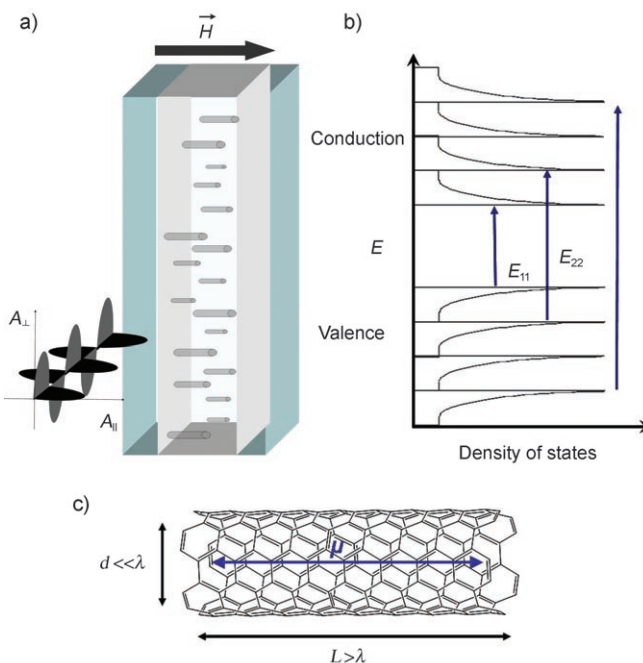


**Figure 1.** Orientation of nanotubes using a weak magnetic field. a) Nanotubes align parallel to the magnetic field ( $H=0.1$  T), which is at right angles to the incident light. The two planes of polarized light  $A_{\perp}$  and  $A_{\parallel}$  used to obtain the linear dichroism spectra are also shown. b) The electronic spectroscopy of carbon nanotubes are characterized by transitions between the van Hove singularities in the density of states, for example,  $E_{11}$ . These unique spectroscopic properties arise from the enormous aspect ratio (c), which approaches the behavior of a one-dimensional solid.

therefore its intensity, is not only governed by the energy but also the polarization of the incident photon. This is described by the transition dipole moment,  $\vec{\mu}$ . The theory behind the electronic transitions of carbon nanotubes implies that their transition moments are oriented mostly parallel to the nanotube long axis. These transitions are strongly allowed and dominate the absorption spectrum. It has, however, also been predicted<sup>[11]</sup> that there are transitions which lie perpendicular to the nanotube axis, and these have been seen by Rodger et al.<sup>[12,13]</sup> These transitions lie at higher energy, as may be expected, as they cannot avail of the extensive delocalization afforded by the  $\pi$  system of the nanotubes. Polarized light spectroscopy should therefore be a perfect tool to give added insight to the electronic structure of carbon nanotubes.

Linear dichroism is a technique whereby an oriented molecule will interact preferentially with certain plane-

[\*] J. Tumpane, Prof. B. Nordén  
Department of Chemical and Biological Engineering/  
Physical Chemistry  
Chalmers University of Technology  
Kemivägen 10, 41296 Gothenburg (Sweden)  
Fax: (+46) 317-723-858  
E-mail: tumpane@chalmers.se

Dr. N. Karousis, Prof. N. Tagmatarchis  
Theoretical and Physical Chemistry Institute  
National Hellenic Research Foundation  
48 Vass. Constantinou Avenue, 11635 Athens (Greece)

[\*\*] This project was part-funded by the European Commission's Sixth Framework Programme (Project reference AMNA, contract no. 013575) (J.T.) and the EURYI award (N.T.). We gratefully acknowledge Prof. Johan Bergenholtz (Gothenburg University) for help with rheology measurements and Prof. Hisanori Shinohara (Nagoya University, Japan) for some of the AFM measurements.

Supporting information for this article, including synthetic and experimental details, is available on the WWW under <http://dx.doi.org/10.1002/anie.200801548>.

polarized light depending on how the transition moments lie with respect to the direction of orientation and the incident polarized light. Important structural information can be gained about the molecule, and the technique has given powerful results for scales ranging from small organic molecules to large biomolecules, such as DNA and proteins.<sup>[14]</sup> The geometry of interactions between molecules can also be determined. Linear dichroism is defined as:

$$LD = A_{\parallel} - A_{\perp} \quad (2)$$

but a more useful concept is the reduced linear dichroism,  $LD^R$ :

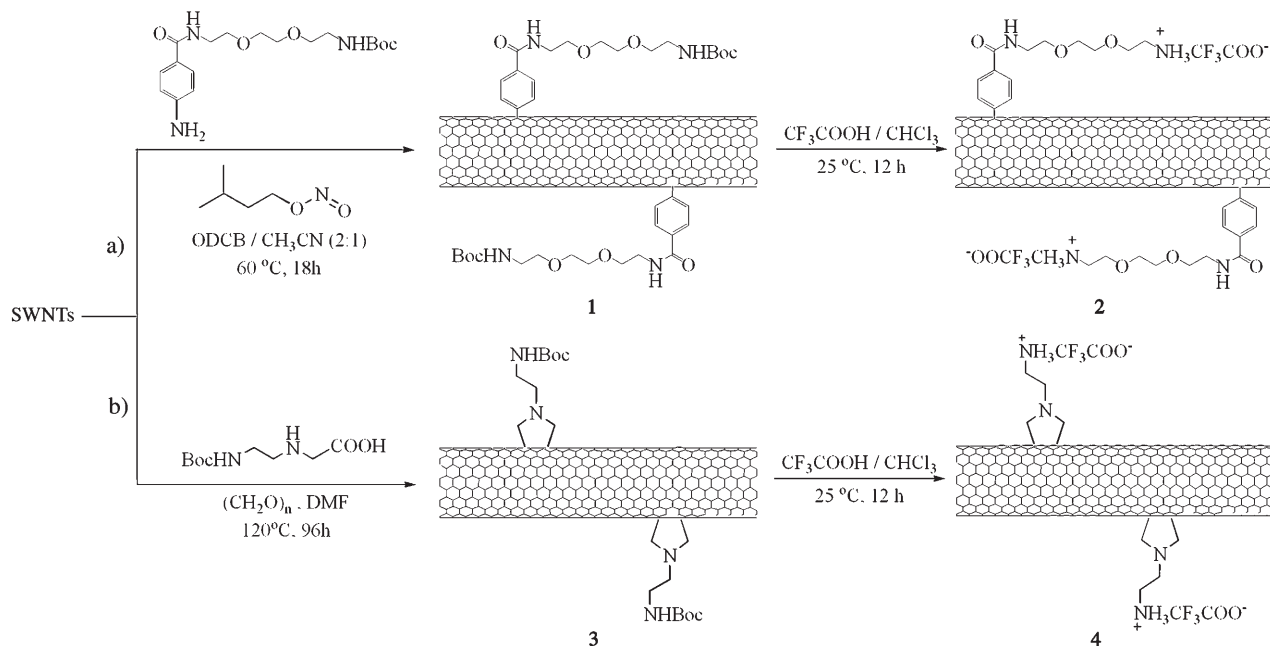
$$LD^R = \frac{A_{\parallel} - A_{\perp}}{A_{\text{iso}}} = \frac{3}{2} S(3 \cos^2 \alpha - 1) \quad (3)$$

for a uniaxial system where  $\alpha$  is the angle between the transition moment and in this case the nanotube long axis.  $S$  is an orientation factor and is 0 for a completely isotropic system and 1 for a perfectly ordered system.

To obtain accurate spectroscopic information, it is important that the carbon nanotubes are solubilized. Bundling of carbon nanotubes is an unavoidable occurrence and is one of the greatest obstacles to harnessing their potential. Solubility can be increased by functionalization of SWCNTs. An effective form of functionalization, introduced by Tour et al.,<sup>[15–18]</sup> consists of the thermal reaction of aryl diazonium compounds, generated in situ, with SWCNTs. This method allows the introduction of aryl groups onto the side walls of the SWCNTs, and has the advantages of solubilization enhancement and the wide variety of the substituted aryl compounds that can be used. High-pressure CO conversion (HiPco) SWCNTs were thus functionalized with *tert*-butyl-2-[2-(4-aminobenzamido)ethoxy]ethoxy]ethylcarbamate

(Scheme 1 a). Water-soluble functionalized SWCNT material **2** is obtained by this procedure. Substantial modification of the nanotubes may, however, break the extensive  $\pi$  delocalization and lead to an eventual disappearance of the electronic fine structure. Alternatively, 1,3-dipolar cycloaddition of azomethine ylides, generated in situ upon thermal condensation of paraformaldehyde and 2-[2-(*tert*-butoxycarbonyl)ethylamino]acetic acid (Scheme 1 b, introduces numerous fused pyrrolidine rings onto the skeleton of SWCNTs.<sup>[19]</sup> Importantly, a modified workup procedure, based on a similar functionalization of carbon nanohorns with azomethine ylides is applied, leading to the isolation of pyrrolidine-functionalized SWCNTs free from organic polymeric impurities.<sup>[20]</sup> However, as UV/Vis/NIR spectroscopy revealed, the presence of the characteristic van Hove singularities are retained, showing a low degree of functionalization with this technique. Characterization of the functionalized SWCNTs materials **1** and **3** by thermogravimetric analysis (TGA), transmission electron microscopy (TEM), and UV/Vis, Raman, and attenuated total reflection IR spectroscopy (see the Supporting Information, Figures S1–S5) unambiguously verifies the success of both functionalization methods.

Iron catalyst impurities remain in trace amounts for nanotubes produced by the HiPco process.<sup>[21]</sup> It is important to recognize that closely spaced amounts of a strongly paramagnetic material may itself have a preferred orientation in the magnetic field. Thus, the HiPco SWCNTs were first purified according to literature procedure,<sup>[15]</sup> and then functionalized as described above. As expected, in the TEM pictures the presence of significant quantities of iron particles is not seen, and TGA analysis (Supporting Information, Figure S1) shows that at most 10 % w/w iron catalyst remains, and normally 1–2 %. We are therefore satisfied that the overriding affect is due to the nanotubes themselves, although we do not wish to rule out a contribution from any



**Scheme 1.** Functionalization of SWCNTs by a) diazonium salts and b) azomethine ylides, both generated in situ. Boc = *tert*-butyloxycarbonyl, ODCB = 1,2-dichlorobenzene.



impurities.<sup>[10]</sup> It has also been shown that the intentional addition of larger amounts of magnetic particles is necessary for magnetic orientation at field strengths up to 1 T.<sup>[10,22]</sup>

The large aspect ratio of carbon nanotubes ( $\mu\text{m}$  lengths vs. nm diameters) is responsible for the directed nature of the unique properties of the SWCNTs and is also even the determining factor in their orientation. Therefore, the advent of soluble SWCNTs in which bundling is less of a problem will give rise to more extreme aspect ratios, facilitating both an increase in the magnetic susceptibility anisotropy  $|\chi_{\parallel} - \chi_{\perp}|$  and a decrease in the rotational diffusion constant  $D_{\text{R}}^{\perp}$  about the two perpendicular axes to the nanotube long axis owing to its cubic dependence on length. Both factors make the ease of orientation much greater. The rigid-rod model of Tirado and de la Torre [Eq. (4)] clearly shows this relationship, where  $L$  is the rod length and  $p$  the aspect ratio of the rod ( $L/d$ ).<sup>[23]</sup> The factor  $\delta_{\perp}$  is a power series in  $p^{-1}$  and approximates as  $-0.662$  as  $p$  becomes extreme.

$$D_{\text{R}}^{\perp} = \frac{3k_{\text{B}}T}{\pi\eta L^3}(\ln p + \delta_{\perp}) \quad (4)$$

Aligned nanotubes will have characteristic relaxation times, which are determined by the diffusion constants, when the external magnetic field is switched off. The decay of the orientation parameter,  $S$ , can be given as:

$$S = S_0(A_1 e^{-\frac{t}{\theta_1}} + A_2 e^{-\frac{t}{\theta_2}}) \quad (5)$$

where  $S_0$  is the initial orientation in the magnetic field, and the correlation times  $\theta_1$  and  $\theta_2$  are then analogous to the depolarization correlation times obtained in, for example, time-resolved fluorescence anisotropy and light-scattering measurements.<sup>[24]</sup>  $\theta_1^{-1}$  and  $\theta_2^{-1}$  correspond to  $6D_{\text{R}}^{\perp}$  and  $4D_{\text{R}}^{\perp} + 2D_{\text{R}}^{\parallel}$ , respectively. In this case the contribution from  $D_{\text{R}}^{\parallel}$  (the rotational diffusion constant about the long axis) will be several orders of magnitude greater than  $D_{\text{R}}^{\perp}$ . This effect greatly decreases  $\theta_2$  (calculated to be  $< 1$  ms), so that it is not observable on the timescale used herein.

The linear dichroism spectra (Figure 2) show that the fine structure of the nanotube electronic transitions is much more evident in DMF than in aqueous solution, which is not surprising, as the nanotubes are much better dispersed in the organic solvent (see the Supporting Information, Figure S6, for dynamic light scattering measurements). Orientation is, however, achieved in all cases using the magnetic orientation, and the transitions between 300 and 800 nm are strongly positive. In fact, magnetic orientation in DMF gives an  $\text{LD}^{\text{R}}$  value of up to 2 (compared to a maximum value of 3 (Equation 3) for all transitions in this range, indicating both that the orientation factor  $S$  is very high (in this case 0.66) and that the transitions all lie parallel or near-parallel with the nanotube long axis, as has been predicted. Such high orientation factors are rarely obtained in solution.<sup>[24]</sup> Corresponding  $\text{LD}^{\text{R}}$  and isotropic absorption spectra are given in the Supporting Information, Figure S7–S9.

In contrast, the higher energy transitions between 170 and 300 nm are negative, indicating that they are at an angle  $\alpha > 54^\circ$  from the nanotube axis. Two important points are that

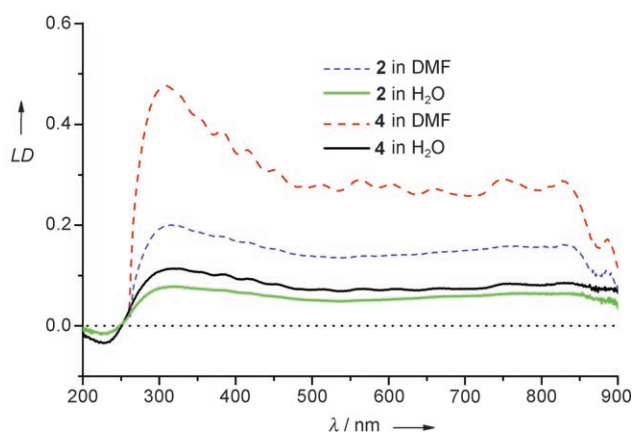


**Figure 2.** Linear dichroism spectra of SWCNTs that are lightly (**4**) and heavily (**2**) functionalized with ammonium groups, acquired in water (solid lines) and DMF (broken lines). The positive signals above 260 nm clearly show the electronic transitions are polarized parallel to the nanotube axis, whereas the negative signals below 260 nm show that some high energy transitions traverse that axis. Spectra are normalized with respect to concentration.

there is no fine structure apparent in this region of the spectrum, and that the absolute value is less than expected, that is, the angle is not  $90^\circ$ , indicating that these transitions may exhibit quite a lot of lateral character. It is important to remember however that effects of scattering<sup>[24]</sup> and possible overlap of the transitions may exaggerate this apparent decrease. The fact that no fine structure is evident for these transitions leads us to assume that either they are very close-lying in energy (that is, masked by spectral overlap), or are not as discrete as the van Hove transitions, and most likely a combination of both factors. The last possibility, is alluded to in the literature,<sup>[11]</sup> as the possibility for extensive delocalization is very limited. Both lightly (**4**) and more heavily functionalized nanotubes (**2**) were used and it is clear that, although just retained, the fine-structure is greatly reduced by more extensive modification and thus disruption of the  $\pi$  electron system. The level of alignment is, however, no better, and in fact worse than for **4**. It has been suggested that significant disruption of the  $\pi$  system will lead to weaker magnetic susceptibilities.<sup>[5]</sup> The solubility difference between the SWCNTs in both water and DMF is also reflected in the levels of orientation achieved, in which the bundles formed in aqueous solution are not as easily aligned.

Relaxation measurements with a time-resolution limit of 20 ms were performed to follow the decay of the  $S$  factor when the magnetic field is switched off (Figure 3). This was monitored at several wavelengths corresponding to the peaks seen for material **4** in the DMF spectrum in Figure 2. In each case, the data could be fitted with three exponentials (see the Supporting Information, Figures S10–11), one of which can be accounted for as the instrument response time (437 ms). In DMF, correlation times of 167 ms and 1.5 s were obtained, and increasing the viscosity to 38 cP with poly(methyl methacrylate) (PMMA, 5 % w/w in DMF solution), the corresponding values were increased to 5 s and 25 s, respectively. These values of  $\theta_1$  are then used to obtain the apparent  $D_{\text{R}}^{\perp}$ , and substitution into Equation 4 gives an estimate of the

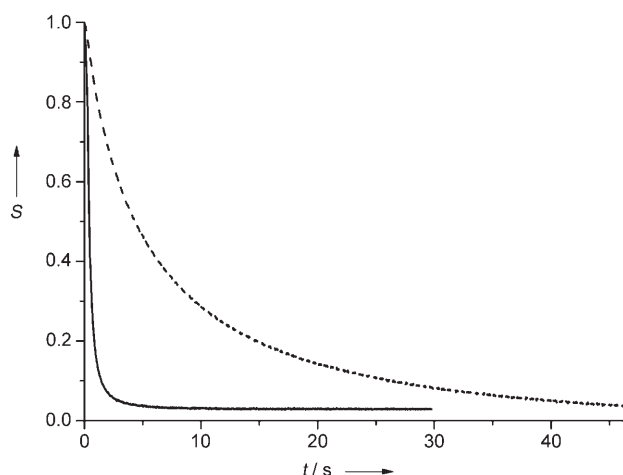


**Figure 3.** Linear dichroism relaxation study on **4** in DMF (solid line,  $\eta = 0.92$  cP) and in a viscous 5 % solution of PMMA in DMF (broken line,  $\eta = 38$  cP). The decay of the orientation parameter  $S$  is related to the rotational diffusion constant  $\theta_1$  and an estimate of the average nanotube length  $L$ ; see text for details.

nanotube lengths. Assuming an extreme aspect ratio  $p$  of 1000 gives an average length of the nanotubes of 3–6  $\mu\text{m}$  in DMF and 2.5–4.6  $\mu\text{m}$  in PMMA/DMF. These lengths are comparable to those observed in AFM measurements (1–5  $\mu\text{m}$ , diameter 10 nm; see the Supporting Information, Figures S12,13) at the same concentrations, although the individual tubes are approximately 1  $\mu\text{m}$  long and 1 nm in diameter. It would therefore appear that these modified SWCNTs form long thin ropes rather than bundling, which will contribute to both better alignment through an exaggeration of the magnetic susceptibility and a decreased diffusion constant arising from the rather long apparent lengths. Similar decays were obtained at all wavelengths, showing that the length of nanotubes has little effect on the electronic properties, such as wavelength, which are thus mostly determined by the chirality, as expected.

The disparity between the two media can partly be attributed to the lack of control over temperature and the accuracy in determining the real viscosity between the two measurements, but may also be due to shorter nanotubes aligning in the more viscous medium because of the dependence of the diffusion constant on the viscosity [Eq. (4)].

In summary, we have demonstrated the orientation of SWCNTs using very weak magnetic fields, which is a significant breakthrough as it shows that physical manipulation and therefore control of certain intrinsic physical properties of nanotubes is possible using a simple electromagnet. The use of modified nanotubes to achieve solubility to exploit the true aspect ratio and avoid bundling but instead allow rope formation is clearly seen. Furthermore, linear dichroism with high-level orientation in the magnetic field allows the characterization of both the electronic structure of

carbon nanotubes and, more importantly, the interaction of small molecules with the SWCNTs.

Received: April 3, 2008

Published online: June 11, 2008

**Keywords:** linear dichroism · magnetic properties · nanotechnology · nanotubes · orientation

- [1] J. Lagerwall, G. Scalia, M. Haluska, U. Dettlaff-Weglikowska, S. Roth, F. Giesselmann, *Adv. Mater.* **2007**, *19*, 359–364.
- [2] M. Fujiwara, M. Fukui, Y. Tanimoto, *J. Phys. Chem. B* **1999**, *103*, 2627–2630.
- [3] T. Suda, S. Ueno, *IEEE Trans. Magn.* **1994**, *30*, 4713–4715.
- [4] B. W. Smith, Z. Benes, D. E. Luzzi, J. E. Fischer, D. A. Walters, M. J. Casavant, J. Schmidt, R. E. Smalley, *Appl. Phys. Lett.* **2000**, *77*, 663–665.
- [5] J. E. Fischer, W. Zhou, J. Vavro, M. C. Llaguno, C. Guthy, R. Haggenueller, M. J. Casavant, D. E. Walters, R. E. Smalley, *J. Appl. Phys.* **2003**, *93*, 2157–2163.
- [6] I. W. Chiang, B. E. Brinson, A. Y. Huang, P. A. Willis, M. J. Bronikowski, J. L. Margrave, R. E. Smalley, R. H. Hauge, *J. Phys. Chem. B* **2001**, *105*, 8297–8301.
- [7] H. Ajiki, T. Ando, *J. Phys. Soc. Jpn.* **1994**, *63*, 4267–4267.
- [8] H. Ajiki, T. Ando, *J. Phys. Soc. Jpn.* **1993**, *62*, 2470–2480.
- [9] X. K. Wang, R. P. H. Chang, A. Patashinski, J. B. Ketterson, *J. Mater. Res.* **1994**, *9*, 1578–1582.
- [10] K. Kordas, T. Mustonen, G. Toth, J. Vahakangas, A. Uusimäki, H. Jantunen, A. Gupta, K. V. Rao, R. Vajtai, P. M. Ajayan, *Chem. Mater.* **2007**, *19*, 787–791.
- [11] A. Gruneis, R. Saito, G. G. Samsonidze, T. Kimura, M. A. Pimenta, A. Jorio, A. G. Souza, G. Dresselhaus, M. S. Dresselhaus, *Phys. Rev. B* **2003**, *67*, 165402.
- [12] J. Rajendra, M. Baxendale, L. G. D. Rap, A. Rodger, *J. Am. Chem. Soc.* **2004**, *126*, 11182–11188.
- [13] J. Rajendra, A. Rodger, *Chem. Eur. J.* **2005**, *11*, 4841–4847.
- [14] K. Frykholm, K. Morimatsu, B. Nordén, *Biochemistry* **2006**, *45*, 11172–11178.
- [15] C. A. Dyke, J. M. Tour, *J. Phys. Chem. A* **2004**, *108*, 11151–11159.
- [16] J. L. Hudson, M. J. Casavant, J. M. Tour, *J. Am. Chem. Soc.* **2004**, *126*, 11158–11159.
- [17] B. K. Price, J. L. Hudson, J. M. Tour, *J. Am. Chem. Soc.* **2005**, *127*, 14867–14870.
- [18] J. J. Stephenson, J. L. Hudson, S. Azad, J. M. Tour, *Chem. Mater.* **2006**, *18*, 374–377.
- [19] V. Georgakilas, K. Kordatos, M. Prato, D. M. Guldi, M. Holzinger, A. Hirsch, *J. Am. Chem. Soc.* **2002**, *124*, 760–761.
- [20] N. Tagmatarchis, A. Maigne, M. Yudasaka, S. Iijima, *Small* **2006**, *2*, 490–494.
- [21] K. Jurkschat, X. B. Ji, A. Crossley, R. G. Compton, C. E. Banks, *Analyst* **2007**, *132*, 21–23.
- [22] F. Stoffelbach, A. Aqil, C. Jerome, R. Jerome, C. Detrembleur, *Chem. Comm.* **2005**, 4532–4533.
- [23] M. M. Tirado, J. G. de la Torre, *J. Chem. Phys.* **1980**, *73*, 1986–1993.
- [24] J. Nordh, J. Deinum, B. Nordén, *Eur. Biophys. J.* **1986**, *14*, 113–122.